Acta Crystallographica Section D
Biological Crystallography
ISSN 0907-4449

Structure of rat transthyretin (rTTR) complex with thyroxine at 2.5 Å resolution: first non-biased insight into thyroxine binding reveals different hormone orientation in two binding sites

Andrzej Wojtczak,[a] Vivian Cody,[b]* Joseph R. Luft[b] and Walter Pangborn[b]

[a]Institute of Chemistry, Nicolas Copernicus University, 87-100 Torun, Poland, and [b]Hauptman–Woodward Medical Research Institute Inc., 73 High Street, Buffalo, NY 14203, USA

Correspondence e-mail: cody@hwi.buffalo.edu

Received 4 December 2000
Accepted 5 May 2001

PDB Reference: rat transthyretin complex with thyroxine, 1ie4.

The first observation of the unique environment for thyroxine (T_4) binding in tetrameric rat transthyretin (rTTR) is reported as determined by X-ray diffraction. These data revealed different modes of hormone binding in the two unique hormone-binding sites in the rat TTR tetramer channel. Differences in the orientation of thyroxine and the position of water molecules in the two binding sites further suggest a mechanism for the docking pathway of the hormone into the channel of TTR. Crystals of the rat transthyretin–thyroxine complex are isomorphous with those reported for apo rTTR and crystallized in the tetragonal space group $P4_32_12$ with four independent TTR monomeric subunits in the asymmetric part of the crystal lattice. Data were collected to 2.5 Å resolution and the structure was refined to $R = 20.9\%$ for 15 384 data in the resolution range 12–2.5 Å. Similar to human TTR, the rat protein is also a 54 000 Da tetramer with four identical polypeptide chains of 127 amino-acid residues. Of the 22 amino-acid residues which differ between the human and rat sequences, none are in the thyroxine-binding domains. Analysis of these structural data reveals that the tertiary structure is similar to that of hTTR, with only small differences in the flexible loop regions on the surface of the structure. Conformational changes of the amino acids in the channel result in a hydrogen-bonded network that connects the two binding domains, in contrast to the hydrogen bonds formed along the tetramer interface in the apo transthyretin structure. These changes suggest a mechanism for the signal transmission between thyroxine-binding domains.

1. Introduction

In man, transthyretin (hTTR, prealbumin) is one of three serum proteins which transports thyroid hormones through the general circulation and is responsible for binding about 20% of the plasma thyroxine (3,5,3′,5′-tetraiodo-L-thyronine; T_4) (Braverman & Utiger, 2000). In rat and other lower vertebrates, transthyretin is the primary serum thyroid hormone-transport protein and thus has a greater physiological role than it does in man (Robbins, 2000; Davis *et al.*, 1970). Rat transthyretin (rTTR) has 85% sequence homology with the human protein and has 22 amino-acid changes in the 127 amino-acid residue monomers (Sundelin *et al.*, 1987; Pettersson *et al.*, 1989) (Figs. 1 and 2). Most of the sequence differences occur in peripheral loop regions, while the hormone-binding domain is strictly conserved. The hormone-binding constants K_a are similar to those for human TTR (Navab *et al.*, 1977). Numerous TTR variants related to familial amyloid polyneuropathy (FAP) are unstable and form

fibrils that are deposited in different organ tissues. The binding of thyroxine or other ligands stabilizes the amyloidogenic TTR variants (Miroy *et al.*, 1996; Klabunde *et al.*, 2000). Knowledge of the thyroid hormone-binding process might be useful in the treatment of patients affected with FAP.

Structural data for wild-type and most mutant complexes of human TTR have two independent monomeric β-barrels (*A* and *B*) in the asymmetric unit of the orthorhombic $P2_12_12$ crystal lattice (Klabunde *et al.*, 2000; Blake *et al.*, 1978; Blake & Oately, 1977; De La Paz *et al.*, 1992; Cody *et al.*, 1991; Ciszak *et al.*, 1992; Wojtczak *et al.*, 1992, 1993, 1996; Damas *et al.*, 1996; Ghosh *et al.*, 2000; Petrassi *et al.*, 2000; Steinrauf *et al.*, 1993; Hamilton *et al.*, 1993; Terry *et al.*, 1993; Schormann *et al.*, 1998).

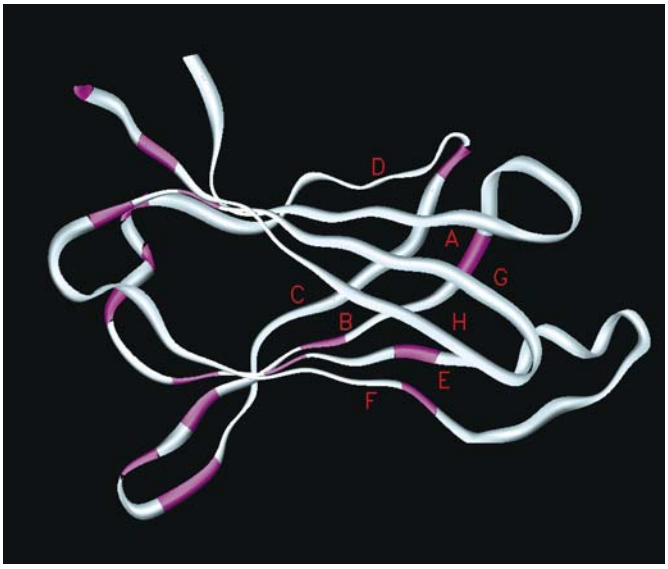

Figure 1
The rat transthyretin monomer with sequence differences between rat and human TTR marked in magenta. β-sheets *A*–*H* are labeled. Prepared with *SETOR* (Evans, 1993).

```
   1                10                20                30                40
h  G P T G T G E S K C P L M V K V L D A V R G S P A I N V A V H V F R K A A D D T
r     G   A                                    V D       K     K   T     G S
  41                50                60                70                80
h  W E P F A S G K T S E S G E L H G L T T E E N F V E G I Y K V E I D T K S Y W K
r                    A                   D   K   T     V   R     L
  81                90                100               110               120
h  A L G I S P F H E H A E V V F T A N D S G P R R Y T I A A L L S P Y S Y S T T A
r                    Y                     H   H
  121         127
h  V V T N P K E
r     S     Q N
```

Figure 2
Sequence comparison between human (h) and rat (r). Only those residues in rat that differ from human are noted.

The only exceptions are the monoclinic forms for the low-resolution structure of apo Leu55Pro TTR (Sebastião *et al.*, 1996, 1998, 2000) and an apo hTTR (Wojtczak *et al.*, 2001). The two independent monomers of the orthorhombic lattice are assembled around a central channel such that the tetramer has molecular 222 symmetry. The independent monomers *A* and *B* are related by a pseudo-twofold symmetry axis parallel to the crystallographic *b* axis. In most hTTR structures, the crystallographic twofold axis is coincident with the channel axis and results in twofold symmetry for each of the ligand-binding sites formed by pairs of monomers (*A*–*A*′ and *B*–*B*′) positioned across the channel axis (Fig. 3). Because of the lack of such molecular symmetry for thyroid hormone and its analogs, the interpretation of the ligand-binding interactions in hTTR has been hampered by the presence of twofold-averaged electron density in the channel representing the two symmetry-related orientations of the bound ligand. Therefore, all reported human transthyretin ligand complexes show a 50% disorder in the occupation of the binding domain (Klabunde *et al.*, 2000, Blake & Oately, 1977; De La Paz *et al.*, 1992; Cody *et al.*, 1991; Ciszak *et al.*, 1992; Wojtczak *et al.*, 1992, 1993, 1996; Damas *et al.*, 1996; Ghosh *et al.*, 2000; Petrassi *et al.*, 2000). Similar to human TTR, the structure of chicken transthyretin (Sunde *et al.*, 1996) also has two monomeric subunits in the asymmetric part of its hexagonal crystal lattice. Data for the structure of the Leu55Pro variant of hTTR indicated two types of substructures in the asymmetric unit – a symmetrical dimer and an independent tetramer (Sebastião *et al.*, 1996, 1998, 2000). In contrast, the reported structure of apo rat TTR (Wojtczak, 1997) is the only structure of transthyretin that has a complete functional tetramer (monomeric subunits *A*–*D*) in the asymmetric unit of the lattice. The *A* and *B* monomers of rTTR are equivalent to the hTTR *A* and *B* subunits, while the *C* and *D* subunits correspond to the *A*′ and *B*′ monomers of the human TTR structures (Fig. 3) but are not related to *A* and *B* by a crystallographic twofold as in the hTTR structures. Thus, the binding domains of the hTTR structures are characterized by identical geometry and intermolecular interactions. On the other hand, the rTTR tetramer channel had no crystallographic twofold symmetry that would impose such constraints on the ligand binding. Therefore, it was expected that the structure of rTTR–ligand complexes would reveal much greater details of the hormone binding in the transthyretin channel.

The aim of this research was to study the details of thyroxine interactions in rat transthyretin, the role of the 22 sequence differences between human and rat TTR in the thyroxine binding and the contribution of the unique tetrameric environment to affinity differences in two binding sites.

2. Experimental

Pooled rat sera were obtained from Pel-Frez (Rogers, AZ, USA) and purified using a modified human transthyretin protocol (Tritish, 1972). The complex crystal suitable for data collection was obtained by cocrystallization of rat TTR and thyroxine from 55–65% ammonium sulfate, 0.1 *M* acetate buffer pH 5.0 using the hanging-drop technique with HANGMAN (Luft *et al.*, 1992; Luft & DeTitta, 1992). 5 µl protein solution was placed over the reservoir of 60% ammonium sulfate, 0.1 *M* acetate buffer pH 5.0. Area-detector data were collected on a Rigaku R-AXIS II imaging-plate system with a Rigaku 200 rotating-anode source from a 0.2 × 0.2 × 0.6 mm crystal at room temperature (293 K). The crystals were tetragonal, space group $P4_32_12$, with a complete tetramer in the asymmetric unit of the crystal lattice, which had unit-cell parameters a = 82.53, c = 161.84 Å. This lattice differs by less than 0.03% from that reported for the apo rTTR structure (Wojtczak, 1997). Of the 83 761 reflections collected, 18 890 were independent (93.8% completeness to 2.5 Å), with an R_{sym} of 10.6%. The highest resolution shell was 82% complete. The average I/σ ratio was 6.0 for all data.

The complex is isostructural with the apo rTTR structure whose coordinates were used for initial phasing of the electron-density maps. The orientation of thyroxine was determined from the 'complex − native' difference maps calculated with *PHASES* (Furey & Swaminathan, 1996). The model was initially refined with *PROLSQ* (Hendrickson & Konnert, 1980; Finzel, 1987; Smith, personal communication) and *X-PLOR* 3.851 (Brünger, 1992) using reflections of resolution higher than 8.0 Å. The model was verified by a series of omit electron-density maps using *CHAIN* (Sack, 1988) and *O* (Jones *et al.*, 1991; Jones & Kjeldgaard, 1997).

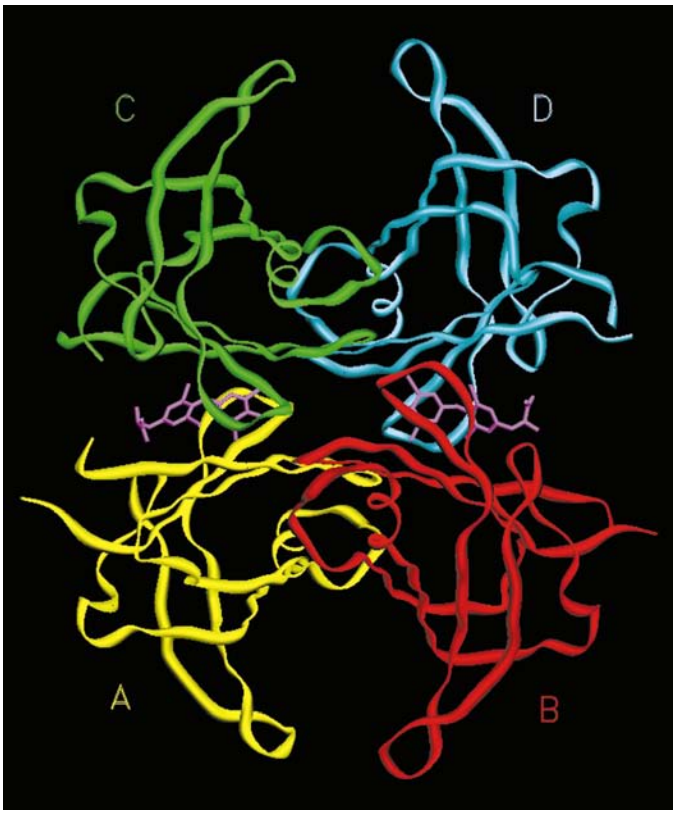

Figure 3
The rat TTR–T_4 complex structure illustrating the two thyroxine (magenta) binding domains, with the monomeric subunits indicated by *A*, *B*, *C* and *D*. In human TTR the twofold related pairs are formed by dimers *A* and *C* (human *A*′) and *B* and *D* (human *B*′). Prepared with *SETOR* (Evans, 1993).

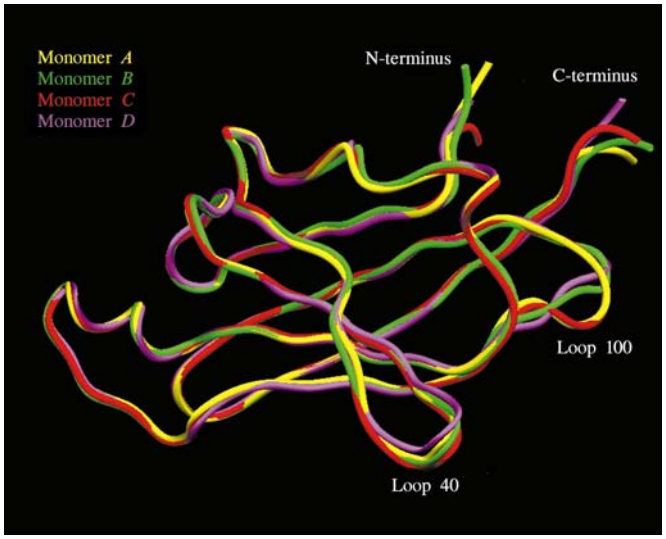

Figure 4
The superposition of the four monomers of rTTR showing the similarity between *A* and *C* as well as *B* and *D* monomers. The β-barrel core of all subunits is rigid. Also shown are the flexible loop regions near residues 40 and 100. Prepared with *SETOR* (Evans, 1993).

Figure 5
The definition of halogen-binding pockets P1, P2 and P3 in transthyretin, highlighting residues that are in contact with thyroxine. Prepared with the program *SETOR* (Evans, 1993).

Final refinement was carried out using *CNS* (Brunger *et al.*, 1998) with the maximum-likelihood target, σ_A-weighted maps and bulk-solvent correction and resulted in $R = 20.98\%$ for 15 384 data in the resolution range 12.0–2.5 Å and $R_{free} = 27.5\%$ for 1147 reflections (7% of data). Since there was no interpretable density for residues 1–7, the structure consists of residues 8–127 for each monomer (*A*–*D*), two thyroxine ligands bound in different orientations in the unique binding sites *AC* and *BD* and 172 water molecules. The final structure also accounts for the disordered positions of the side chains of Met213 and Arg621. Conformational statistics show that 85.6 and 14.4% of the residues are positioned in the most favorable and allowed regions of the Ramachandran plot, respectively, as calculated with the program *PROCHECK* (Laskowski *et al.*, 1993). The superposition of the four monomers of rTTR on hTTR reveals little conformational difference in their β-sheet structures (Fig. 4). The data-collection and final refinement statistics are summarized in Table 1 and the coordinates of rTTR have been deposited with the PDB.

Table 1
Data-collection and refinement statistics for the structure of rat TTR–T_4.

Space group	$P4_32_12$
Measured reflections (82.5–2.5 Å)	83761
Independent reflections	18890
Mean I/σ	13.0/2.1
R_{mer} (%)	10.6
Resolution (Å)	12.0–2.5
Unique reflections	18890
Reflections used (2.5σ)	16558
Reflections used (%)	83.5
R factor (15 384 reflections)	0.209
R_{free} (1174 reflections)	0.275
Protein atoms	3707
Ligand atoms	48
Water molecules	172
B factor (Wilson statistics) (Å^2)	17.4
B factor (protein) (Å^2)	17.38
B factor (water) (Å^2)	18.92
R.m.s. bond distance (Å)	0.007
R.m.s. angle (°)	1.280
R.m.s. improper angles (°)	1.117
Residues in most favored regions of Ramachandran plot (%)	85.6
Residues in allowed regions (%)	14.4
Positional error estimated from Luzzati (1952) (Å)	0.3

3. Results and discussion

The four independent monomeric subunits (*A*–*D*) of rat TTR constitute the asymmetric unit of the crystal structure. The small differences observed in the geometry of the four rTTR subunits reflect differences in their intermolecular interactions owing to crystal packing. The major differences in main-chain conformation between subunits are found in the flexible regions for residues 34–41 and 98–104, which are fragments that are disordered in the reported crystal structures of human and rat transthyretin. The 98–104 fragment and the N- and C-termini of each monomeric subunit contain numerous charged amino acids (Arg, His) and Gly residues in their sequence (Fig. 2) and may contribute to their observed disorder and thus might be related to the opening and closing of the channel entrance or the recognition and transport of T_4 zwitterion towards the binding site. However, as yet no structural data support this hypothesis.

3.1. Halogen-binding pocket occupation

There are three pairs of halogen-binding pockets (P1–P1′, P2–P2′, P3–P3′) in each hormone-binding site of the TTR tetramer (Fig. 5). The innermost P3 pocket is formed by aliphatic side chains of Ala108, Leu110, Thr119 and Ser117. One surface of the P3 pocket is formed by the main-chain carbonyl and NH groups of Ala108, Ala109, Leu110, Ser117, Thr118 and Thr119. Therefore, this pocket has mixed hydrophobic and polar characteristics, with significant contributions from nucleophilic groups in the polypeptide chains. The middle P2 pocket formed by the side chains of Leu110, Ala109, Lys15 and Leu17 has a hydrophobic character. The carbonyl groups of Ala109, Lys15 and Ala108 form one hydrophilic surface of this pocket. The outer P1 pocket is shaped by the side chains of Thr106, Met13 and Lys15; while being positioned between the strands *A* and *E*, it is separated from the P2 pocket by the side chains of Leu17 and Lys15. The deep cavity between Glu54, Lys15 and Met13 positioned next to the P1 pocket is not filled by any of the ligands in the TTR complexes studied to date. Significant contribution to the ligand binding can come from the charged surface region formed by the side chains of Glu54 and Lys15.

The 'complex − native' electron-density maps, calculated with *PHASES* (Furey & Swaminathan, 1996) and contoured at 5σ above background, revealed four density peaks in the P1 and P1′ outer pockets, the proximal P2 pocket of monomer *A* and the distal P3′ pocket of monomer *C*, and correspond to the T_4 iodine-substituent positions in the *AC* binding site formed by monomers *A* and *C*. Such an orientation is similar to that reported for human TTR–T_4 complex (Wojtczak *et al.*, 1996). The additional density peak observed at the 4σ level could not be interpreted as a phenolic iodine of T_4 in an alternative orientation and thus it was assigned as a water molecule bound in the P3 pocket. The observed density distribution indicates that thyroxine is bound in the *AC* site in a single orientation (refined occupancy 0.40) and does not have the twofold disorder found in the human TTR complex (Wojtczak *et al.*, 1996). The omit map (Fig. 6) shows the hormone molecule is bound in the overall *transoid* conformation and in a skewed −84.3/−8.6° conformation of the ether bridge, similar to the conformation of the thyroxine molecule (Cody, 1980, 1981). The χ_1 and χ_2 torsion angles describing the conformation of the tyrosyl moiety of the hormone are 60.9 and 89.0°, respectively. In this orientation the phenolic hydroxyl group of T_4 hydrogen bonds to the water molecule in P3 pocket of monomer *A* (2.75 Å), which also forms a contact to iodine I3′ (3.41 Å). The second water molecule found in this pocket hydrogen bonds to the first water and to the Ser117 side chain (2.66 and 2.92 Å, respectively). Owing to this interaction, the Ser117 side chain has a different conformation to that found in the apo rTTR (Wojtczak, 1997) and forms a 2.71 Å hydrogen

bond to Ser317 of the second binding site. The carboxylic group of T_4 is positioned close to monomer *C* and forms a 3.61 Å interaction with the Lys415 amino group. The hormone amino group participates in a 4.3 Å contact with the Glu454 carboxylic group. The short contact of 3.07 Å found between I3′ and the Ala109 carbonyl group is consistent with the CSD search for I···O interactions (Cody & Murray-Rust, 1984).

In the *BD* binding site the major electron-density peaks are found in the P3/P3′ and P1/P1′ pockets, corresponding to the hormone phenolic I3′ and I5′ and tyrosyl I3 and I5 substituents, respectively. The fifth density peak in the P2 pocket indicates the position of the water molecule bound between I5′, the Ala309 carbonyl group and the Leu217 backbone N atom. The omit map (Fig. 7) reveals that thyroxine (refined occupancy 0.36) is bound in a twisted conformation (Cody, 1980, 1981) with φ and φ' torsion angles of 100.4 and −42.7°, respectively. The χ_1 and χ_2 torsion angles of the tyrosyl moiety are 178.7 and 73.0°, respectively. The twisted conformation of T_4 permits it to penetrate the binding site deeper than observed for the skewed conformation in the *AC* site. Both the phenolic iodine substituents in the P3/P3′ pockets do not form close contacts with the nucleophilic carbonyl groups of the main chain. The shortest I···O distance to Ala308 and Ala708 is about 3.5 Å owing to the central position of the phenolic ring in the channel. Also, the phenolic hydroxyl group does not form direct interactions with the surrounding Ser317 and Ser717 residues. Instead, both serine residues are involved in polar interactions to Ser117 and Ser517 across the tetramer interface (2.88 and 4.16 Å, respectively). The single water molecule found near Thr319 hydrogen bonds only to thyroxine OH (2.55 Å). The carboxylic group of T_4 interacts with Lys615 (3.37 Å) and a water molecule (2.77 Å). The hormone amino group interacts with the Glu254 carboxyl group of monomer *B* (3.41 Å).

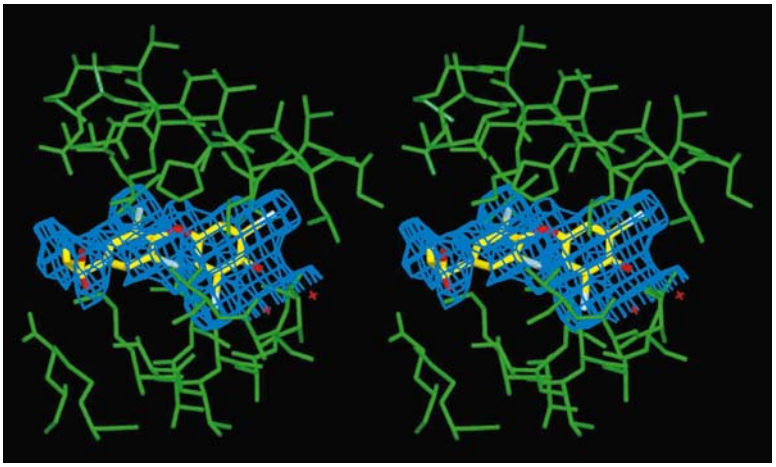

Figure 6
Stereoview of omit electron-density map (1σ) for the *AC* site of the rTTR–T_4 complex, showing T_4 bound in the P2/P3′ orientation and the water molecules (x) in the P3 pocket.

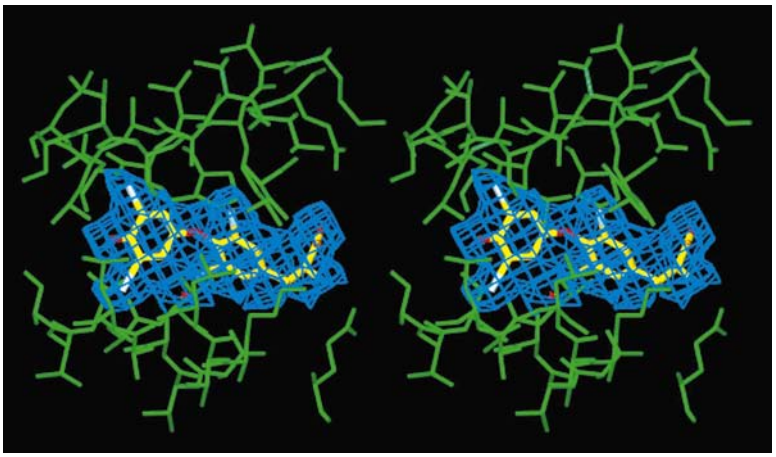

Figure 7
Stereoview of omit electron-density map (1σ) for the *BD* site of the rTTR–T_4 complex, showing the P3/P3′ orientation of T_4 and the water molecule (x) in the P2 pocket.

Comparison of the *AC* and *BD* binding sites in the rTTR–T_4 structure (Fig. 8) reveals that the main-chain conformation is similar in both sites. In the *AC* site the phenolic iodine substituents are positioned in the P2 and P3′ pockets of monomers *A* and *C*, respectively. The pair of water molecules found in the P3 pocket of monomer *A* form hydrogen bonds between the phenolic OH group of T_4 and the Ser117 side chain. There are no similar hydrogen bonds in the *BD* site owing to the P3/P3′ binding of the ligand iodines. The two water molecules are found in P2 pockets (monomers *B* and *D*) and interact with the polar groups of Ala308 and Ala708. Therefore, the Ser317 side chain has a different conformation to Ser117. The deep binding of T_4 in the *BD* site also alters the conformation of Leu310 when compared with its Leu110 equivalent in monomer *A*. Also, the conformations of Thr119 and Thr519 in site *AC* differ from the conformations of Thr319 and Thr719 in site *BD*. The Thr319, in the conformation altered by T_4, forms a 3.36 Å hydrogen bond to Ser115 across the tetramer interface.

In the structures of T_4 complexes with wt hTTR (Wojtczak *et al.*, 1996) and its variants Val30Met (Hamilton *et al.*, 1993) and Ala109Thr (Steinrauf *et al.*, 1993), T_4 occupies a similar position and is bound in the P3/P2′ orientation in both binding sites. This mode of binding is similar to that found in the *AC* site of the rTTR–T_4 complex. However, in these complexes there is no equivalence of the P3/P3′ mode of T_4 binding found in the *BD* site of this complex. The position of water in the P3 pocket of the rTTR *AC* site is close to that of the phenolic iodine of the ligand in P3/P2′ orientation in hTTR, but is shifted slightly towards the tetramer center. The water molecules found in the P2 pockets of the *BD* site also are positioned closer to the channel entrance that the position determined in hTTR for the iodine substituent of the P3′/P2 oriented ligand.

Table 2
Comparison of the side-chain conformation for amino acids in the binding site, as observed upon thyroxine binding to rat TTR.

Amino acid	Apo TTR	Complex
Site *AC*		
Ser115	172.3	171.1
Ser117	33.1	179.3
Thr118	−173.1	−168.5
Leu417	−72.9/89.4	−104.6/49.5
Ser512	−93.7	178.4
Ser517	33.4	81.8
Thr518	179.0	−166.5
Thr519	−173.7	−54.9
Site *BD*		
Leu217	−69.5/−170.4	−65.9/180.0
Leu310	−175.0/55.0	−157.9/−73.4
Ser317	57.6	−58.5
Thr319	−51.7	−78.1
Leu617	−53.6/−169.1	−51.9/−173.8
Ser715	−173.8	−178.3
Thr719	−47.2	−179.0

Since the averaged occupancy of P3/P2′ and P3/P3′ oriented ligands would give the same electron-density distribution with similar solvent structure, the detection of the possible P3/P3′ orientation of T_4 in hTTR complexes was not possible.

Comparison of the *AC* site with the apo rTTR structure (Wojtczak, 1997) shows no significant differences in the side-chain conformations (Table 2). In contrast, the presence of T_4 bound deep in both P3 and P3′ pockets of the *BD* domain results in conformational changes of Leu310, Ser317, Thr319, Leu617 and Thr719 surrounding thyroxine. Also, Lys215 and Lys615 have different conformations and interact with the alanyl moiety of T_4 *via* several water molecules. In the apo rTTR structure all the side chains mentioned above are positioned towards the channel center. Comparison between the hTTR–T_4 complex (Wojtczak *et al.*, 1996) and the rTTR–T_4 complex shows few significant differences in the *AC* site and fewer differences in the *BD* site. Therefore, we conclude that the major conformational changes result from differences in the orientation of thyroxine. The twofold disorder observed in the orthorhombic human TTR complexes does not allow recognition of the new P3/P3′ binding mode of T_4. The only indication of such binding was the cross-phased density map calculated as described in Wojtczak *et al.* (1996).

3.2. Thyroxine binding based on the comparison of human and rat TTR complexes

In all the hTTR complexes reported to date, the ligands have been bound in a binding site composed of a pair of two twofold-related TTR monomers. Therefore, in the structures of human TTR complexes, the twofold averaging of the electron density, as required by the crystallographic symmetry axis along the channel, resulted in the convoluted features of the density maps. The hTTR–T_4 complex obtained by soaking of thyroxine into the TTR crystals (Blake & Oately, 1977) revealed a water molecule positioned in the inner P3 pocket, while the phenolic iodines of the hormone molecule occupied the other inner P3′ and P2 pocket. The structure determination of cocrystallized hTTR–T_4 complex (Wojtczak *et al.*, 1996) revealed that thyroxine binds deeper than in the crystal soaked with hormone; also, no additional peak corresponding to water molecule was present. However, it was impossible to distinguish between the possible P3/P3′ and P2/P3′ binding modes of the hormone. The rat TTR structure reported here has provided the first opportunity to overcome the statistical disorder of the ligand position in TTR and to analyze the details of T_4 binding. In one binding domain, the hormone is bound with the phenolic I atoms bound in the P2/P3′ pocket and with the water molecule positioned deep in the P3 pocket, similar to the structure reported for a hTTR–T_4 complex (Blake & Oately, 1977). In the second binding domain, the phenolic iodines occupy the P3/P3′ pockets and the water molecule was found in the P2 middle pocket, similar to that observed for the cocrystallized complex (Wojtczak *et al.*, 1996). In all these structures the polar interactions of the hormone alanyl moiety with Lys15 and Glu54 were maintained.

The comparison of both human TTR–T_4 complexes with the rat complex reported here suggests a mechanism for thyroxine docking to TTR. In the first step, the electrostatic recognition of the T_4 alanyl moiety by Lys15 and Glu54 positions the hormone at the channel entrance. The ligand then penetrates the set of pockets starting from the outer P1

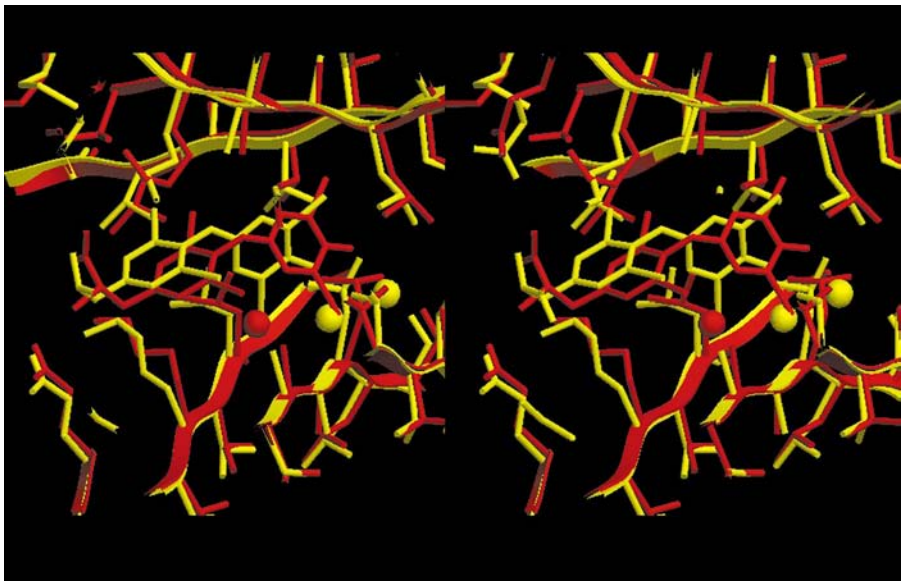

Figure 8
Superposition of the *AC* (yellow) and *BD* (red) sites for the rTTR–T_4 complex, produced with the program *SETOR* (Evans, 1993).

pockets. On the way towards the center of TTR tetramer, the ligand removes the solvent molecules bound in partially hydrophilic P2 and P3 pockets. The first stage was detected in the soaked hTTR–T_4 complex as reported by Blake & Oately (1977) and is similar to that found in the *AC* binding site of this structure. In the second stage, the hormone molecule removes the P3 bound water, positioning its phenolic iodine substituents in P3 and P3′ pockets on the opposite sides of the binding site. The removed water is pushed to the empty P2 pocket. This orientation of the ligand was found in the *BD* site of the reported structure. Finally, the water molecule escapes from the hydrophobic environment of the P2 pocket flanked by the ring system of the hormone. The ligand phenolic iodines are positioned in the P3 or P2 pockets, as indicated by the electron density in the co-crystallized hTTR–T_4 complex structure (Wojtczak *et al.*, 1996).

3.3. Specificity of the TTR ligand-binding pockets

The TTR hormone-binding sites consist of four unique regions: the distal P3 pocket with substantial contribution from nucleophilic hydroxyl and carbonyl groups and aliphatic side chains, the proximal P2 pocket formed by aliphatic side chains and the nucleophilic carbonyl and polypeptide N—H groups exposed, the outer P1 pockets that are exclusively aliphatic and the charged surface region formed by Lys15 and Glu54. The P1 to P3 pockets are located in the grooves between adjacent β-strands and are separated by the amino-acid side chains and the charged path is on the channel surface close to the channel entrance. All of these regions are involved in ligand-binding interactions. Comparative analysis of the TTR complex structures enables one to form conclusions about their contribution to the overall binding energy.

We have determined the crystal structure of hTTR complexes with thyroxine and its analogs 3,3′-diiodo-L-thyronine (3,3′-T_2) and 3′,5′-dinitro-*N*-acetyl-L-thyronine (DNNAT), as well as milrinone (Wojtczak *et al.*, 1992, 1993, 1996) and a flavonoid ligand (Ciszak *et al.*, 1992). The topology of the binding site is such that the iodines of the conformationally constrained T_4 can occupy both P3 and P3′ pockets simultaneously only when T_4 has a twist diphenylether conformation, as found in the *BD* site of the rTTR–T_4 structure. Otherwise, the ligand iodine substituents occupy the distal P3, the proximal P2′ pocket and the two outer P1/P1′ pockets, as found in the *AC* site of this rTTR–T_4 complex or in the hTTR–T_4 complexes. In both orientations the alanyl moiety of T_4 is involved in polar interactions with the charged Lys15 and Glu54 close to the channel entrance. Also, the 3,3′-T_2 I atoms occupy the P2 and P3 pockets and have a skewed conformation similar to T_4, which places the thyronine nucleus across the TTR channel. As was found in both T_4 and 3,3′-T_2 complexes, the iodine substituents bound in the inner P2 and P3 pockets form contacts to nucleophiles such as carbonyl or peptide N—H groups, with the distances being as short as 2.80 Å. The I···O or I···N distances are found to be much shorter than the sum of van der Waals radii; this is consistent with the structural results retrieved from the Cambridge Structural Database (CSD; Cody & Murray-Rust, 1984). The energy of short nucleophile–iodine interactions is similar to that of the weak hydrogen bonds (Kollman *et al.*, 1982). The alternative interactions enable the positioning of the I atoms in either P3/P2′ or P3/P3′ orientation. The interactions of tyrosyl iodines in the hydrophobic P1 pockets result from the ligand anchoring between P3 and P2 pockets and the charged amino acids at the channel entrance and seem to be only of secondary importance for the ligand binding.

If the ligand possesses a greater conformational flexibility, not restricted by two tyrosyl ring substituents, it can adopt different ether-bridge conformations and occupy distal and proximal pockets on the different monomers constituting the binding site, as found in the TTR–3,3′-T_2 complex (Wojtczak *et al.*, 1992). To accomplish this, the ligand is bound across the channel and its skewed conformation is slightly altered. In both cases the iodine substituents may be a target for nucleophile binding.

Ligands in which the ether-bridge conformation is not restricted, such as DNNAT or milrinone, can penetrate the binding site deeper and their substituents are bound in the innermost P3 pockets. In the DNNAT–TTR complex (Wojtczak *et al.*, 1996), the additional factor is the nucleophilic character of the nitro groups. These groups tend to bind to a hydrogen-bond donor, such as Ser117 OG hydroxyl or the polypeptide chain N—H groups. This tendency favors the P3 pocket binding, since only that pocket has the proton-donor groups exposed. Such a preference should also be observed for chloro and, to certain extent, bromo analogs of thyroxine.

The hydrophobic core of the hormones is bound along the aliphatic channel surface, interacting with the side chains separating the halogen-binding pockets. These interactions could be a significant binding contribution in the case of ligands lacking the substitution on their tyrosyl rings, such as DNNAT. In its complex, the ligand tyrosyl moiety is bound along the groove between β-strands *E* and *A* and is significantly shifted from the channel axis. The opposite effect seems to be observed for the TTR–T_4 complex. The rigidity of the molecule and four bulky iodine substituents prevent it from being positioned off the channel axis. The intermediate orientation is observed for 3,3′-T_2, which binds P2′ and P3 pockets across the channel and participates in hydrophobic core interactions with the surrounding aliphatic side chains (Wojtczak *et al.*, 1992). We can hypothesize that by replacing specific I atoms by aliphatic substituents one could decrease the molecule rigidity and change the pocket preferences, which could result in the ligand binding along the channel axis with P1 hydrophobic interactions dominating the binding process. The effect can be quantified by comparing the relative ligand orientation in the TTR channel. The axis of the T_4 molecule, defined across the ligand-ring system as a line between the phenolic ring C4′ and tyrosyl C1 atoms, is almost parallel to the channel axis. In the 3,3′-T_2 complex the angle between these axes is about 10°, while for DNNAT it is approximately 20°.

3.4. Thyroxine-induced changes in the transthyretin binding sites

No significant conformational changes of the polypeptide chain have been detected upon T_4 binding to rat transthyretin. In particular, the rigid β-sheet core of the tetramer does not undergo major conformational adjustments. However, there are several changes in the side-chain conformation of the amino acids constituting the hormone-binding sites. The four water molecules conserved between the native rTTR and its T_4 complex structure have been found at the center of the TTR tetramer, between the four monomer subunits. In the unliganded TTR these water molecules form a network of hydrogen bonds along the tetramer interface, involving Ser117, Ser115 and Ser717 of monomers *A* and *D* as well as Ser312, Ser317 and Ser512 of monomers *B* and *C* (Wojtczak, 1997). The binding of thyroxine in rTTR involves two water molecules found in the P1 pocket of the site *AC*, while the orientation of the phenolic iodines in pockets P1 and P1′ excludes such a water presence in the site *BD*. In the unliganded rat transthyretin structure water molecules have been found in the pockets P3′ and P2 of both the T_4-binding sites. Significant closure of the space between the side chains of Lys15 and its equivalent residues (Lys215, Lys415 and Lys615) was observed on binding T_4. The distance between Lys15 CD atoms across the binding sites *AC* and *BD* are 8.46 and 9.45 Å, and 7.69 and 8.40 Å for the unliganded and T_4-bound rat transthyretin, respectively. The observed differences in the chain conformation and the water positions lead to the proposed model of the T_4-binding mechanism with signal transmission between the binding sites. The numbering of the residues used below to describe the observed changes are kept consistent with the hTTR–T_4 complex structure.

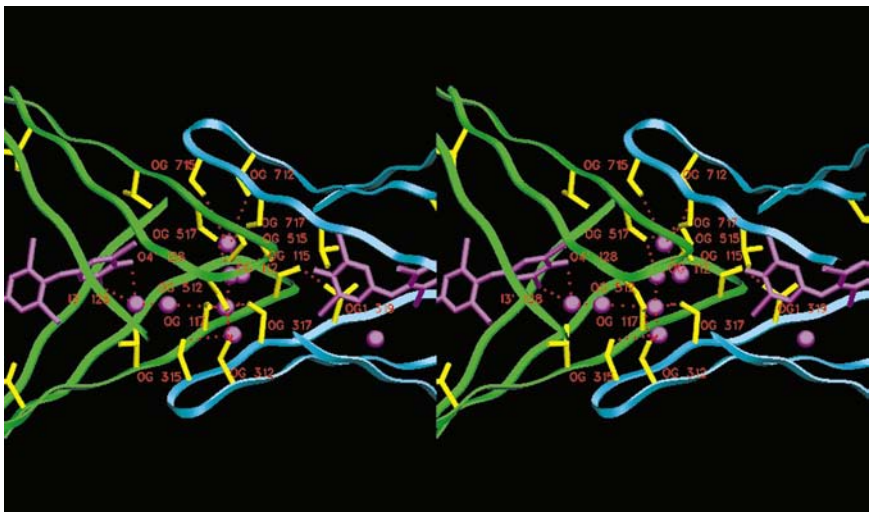

Figure 9
The hydrogen-bond network at the tetramer interface in the rTTR–T_4 complex. Ribbon structures for domain *AC* and *BD* are in green and cyan, respectively, T_4 is in magenta, water molecules are shown as magenta balls, interacting residue side chains are in yellow and hydrogen bonds are in red.

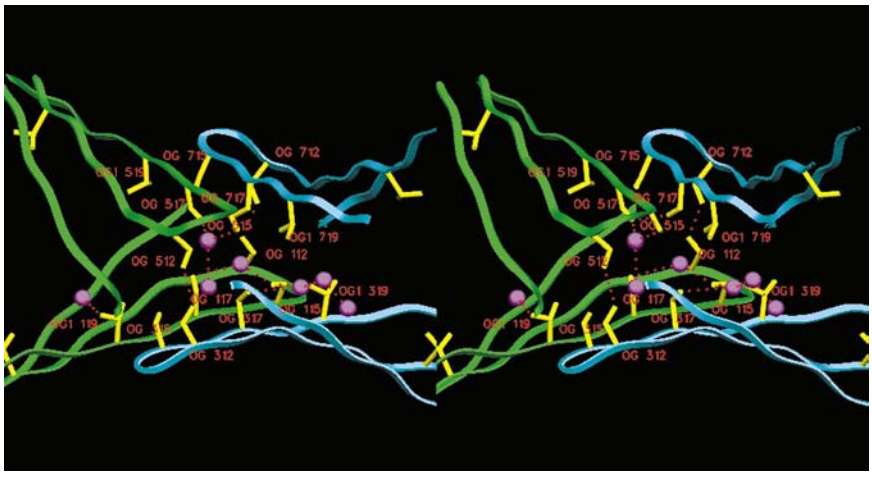

Figure 10
The hydrogen-bond network at the tetramer interface in apo rTTR (Wojtczak, 1997). Ribbon structures for domain *AC* and *BD* are in green and cyan, respectively, water molecules are shown as magenta balls, interacting residue side chains are in yellow and hydrogen bonds are in red.

Upon entering the open channel in which the Lys215 and Lys615 chains are positioned approximately 9 Å apart from each other, thyroxine binds deep in the channel with its phenolic iodines positioned in both P3 and P3′ pockets, which causes reorientation of the Leu310 and Thr319 side chains. The Lys15 side chains move closer by about 1 Å, with their methylene groups forming hydrophobic interactions with the tyrosyl moiety of the hormone. The bulky phenolic iodines then cause the reorientation of the Ser317 and Ser717 side chains, thereby disrupting any hydrogen bonds to solvent inside the binding site and removing the water molecules from the both P2 and P3 pockets. The reorientation of Ser and Thr hydroxyl groups results in the formation of a new hydrogen-bond network directly between Ser317 and Ser117, Thr319 and Ser115, as well as from Thr519 to Ser715 across the interface. The new network of hydrogen bonds between two binding sites replaces the previously existing network of interactions along the interface separating these sites, changes the local polarity and creates the new network of side chains and water interactions (Figs. 9 and 10). The conserved water molecules at the tetramer interface also participate in the new hydrogen-bonding network. The changes in the monomer *A* and *C* Ser side-chain conformations cause a shift of well defined water molecules in the P3′ and P2 pockets of the site *AC* to the halogen-binding pocket P3, where they form hydrogen bonds to hydroxyl and

main-chain carbonyl groups of Ser117 and Thr119. The conformational changes resulting from the ligand binding are transmitted to the second site, also disrupting the hydrogen bonds to the water molecules in the inner pockets. This allows the second T_4 molecule to bind in the empty P3′ and P2 pockets of the second binding site of the transthyretin tetramer. The hormone molecule bound in the second site reconstitutes a hydrogen-bond network and forms a partly polar cavity in the P2 pocket that might contain a water molecule, as observed in the rTTR–T_4 structure.

The proposed mechanism, based on the observed conformational changes, might explain the negative cooperativity of T_4 binding to transthyretin. The presence of two bulky iodine substituents bound in both P2 and P3′ simultaneously seems to be crucial for the Ser and Thr conformational changes and results in the disruption of the existing network of hydrogen bonds with the solvent inside the binding site and the formation of an alternative network of interactions between the altered side chains of both binding sites and the solvent in the second site. The ligand binding to the phenolic I atoms in both the inner P2 and P3′ pockets seems to be more favorable than the P3/P3′ mode of binding, since the iodine interacts with the protein. The binding of water in the P3 pockets is weaker than that found for the P2/P3′ orientation. Also, the latter interactions are mediated by the water molecules easily penetrating the binding sites. For the 3′,5′-dinitro-*N*-acetylthyronine analog (Wojtczak *et al.*, 1996), the Ser117 hydroxyl groups are oriented towards the interior of the binding site and form hydrogen bonds to both nitro groups, which are not able to participate in signal transmission between the sites. The above conclusions are based only on the structural data, since there are no reports on the binding affinities to the first and second ligand molecule to TTR tetramers other than those of thyroxine (Cheng *et al.*, 1977).

The small adjustments of the main-chain conformations are caused by the new network of hydrogen bonds formed upon the T_4 binding. These changes result in slightly altered positions of the side chains of Pro113, Tyr114 and Pro86. These changes, including reorientation of the Thr118, Ser115 and Ser112 hydroxyl groups, result in the altered environment of the Trp79 ring system. The observed changes are consistent with the results of fluorescence studies on the conformational changes in TTR upon thyroxine binding (Gonzalez & Tapia, 1992).

4. Conclusions

We report the first structural details of thyroxine binding in a unique tetrameric TTR environment. The structure of the rTTR–T_4 complex has revealed two different thyroxine-binding modes. In one mode, thyroxine is positioned in the channel with the phenolic iodines bound in the P2 and P3′ pockets of site *AC* with binding interactions mediated by the water molecules positioned in the P3 pocket not containing the T_4 iodine. The second binding site (*B*/*D*) binds the ligand with the phenolic iodines positioned in both P3 and P3′ inner pockets. The water molecule found in the middle P2 pocket mediates the T_4-binding interactions. The different binding of T_4 is possible owing to the conformational changes of the hormone ether bridge and owing to the formation of a 3.07 Å I$\cdots$O interaction to the main-chain carbonyl groups. The different modes of ligand binding also result in different conformations of the side chains forming the channel surface. Also, the difference in the hydrogen-bond network is observed between the complex and the apo rTTR. In the apo rTTR the hydrogen bonds at the tetramer center are formed mainly along the interface between the two binding sites. In the rTTR–T_4 complex, the hydrogen bonds are formed along the channel axis, thereby transmitting the signal from one site to the other. Such changes might be a part of the mechanism of negative cooperativity, which is used to explain the differences in the binding affinity of two hormone-binding sites in transthyretin.

Also, comparison of the soaked hTTR–T_4 complex structure (Blake & Oately, 1977) with the cocrystallized hTTR–T_4 structure (Wojtczak *et al.*, 1996) and the complex reported here suggests a binding pathway for T_4 in transthyretin. The initial position is P2/P3′ as observed in the *AC* site of the investigated complex, as this orientation is the major one in the rTTR. The small conformational changes of the central TTR channel in both sites results in the hormone binding in the P3/P3′ orientation in the secondary site (*BD* in the reported structure). The water molecules bound in the partially polar pockets of the channel are removed by the ligand penetrating the binding site. Despite differences in the orientation of the ligand, its interactions formed by Lys15 at the channel entrance are preserved, suggesting that they are a component of the ligand-recognition mechanism in transthyretin.

This work was supported in part by National Institutes of Health Grants DK 41009 (VC) and Fogarty TW00226 (VC) and the Polish Committee for Scientific Research Grant 6/P203/005/05 and 6/P04A/032/11 (ASW). The authors wish to thank Colin Desnoes for his assistance in the purification of rat TTR, Ilona Wawrzak for crystal-growth experiments and G. D. Smith for making available his set of programs.

References

Blake, C. C. F., Geisow, M. J., Oatley, S. J., Rerat, C. & Rerat, B. (1978). *J. Mol. Biol.* **121**, 339–356.
Blake, C. C. F. & Oately, S. J. (1977). *Nature (London)*, **268**, 115–129.
Braverman, L. E. & Utiger, R. D. (2000). Editors. *The Thyroid, A Fundamental and Clinical Text*, 8th ed. Philadelphia: J. B. Lippincott.
Brünger, A. (1992). *X-PLOR Manual.* New Haven, USA: Yale University Press.
Brunger, A. T., Adams, P. D., Clore, G. M., DeLano, W. L., Gros, P., Grosse-Kunstleve, R. W., Jiang, J.-S., Kuszewski, J., Nilges, M., Pannu, N. S., Read, R. J., Rice, L. M., Simonson, T. & Warren, G. L. (1998). *Acta Cryst.* D**54**, 905–921.
Cheng, S., Pages, R. A., Saroff, H. A., Edeldoch, H. & Robbins, J. (1977). *Biochemistry*, **16**, 3707–3713.
Ciszak, E., Luft, J. & Cody, V. (1992). *Proc. Natl Acad. Sci. USA*, **89**, 6644–6648.
Cody, V. (1980). *Endocrinol. Rev.* **1**, 140–166.

Cody, V. (1981). *Acta Cryst.* B**37**, 1685–1690.
Cody, V. & Murray-Rust, P. (1984). *J. Mol. Struct.* **112**, 189–199.
Cody, V., Wojtczak, A., Ciszak, E. & Luft, J. R. (1991). *Progress in Thyroid Research*, edited by A. Gordon, J. Gross & G. Hennemann, pp. 793–796. Rotterdam: Balema.
Damas, A. M., Ribeiro, S., Lamzin, V. S., Palha, J. A. & Saraiva, M. J. (1996). *Acta Cryst.* D**52**, 966–972.
Davis, P. J., Spaulding, S. W. & Gregerman, R. I. (1970). *Endocrinology*, **87**, 978–986.
De La Paz, P., Burridge, J. M., Oatley, S. J. & Blake, C. C. F. (1992). *The Design of Drugs to Macromolecular Targets*, edited by C. R. Beddell, pp. 119–172. New York: Wiley & Sons.
Evans, S. V. (1993). *J. Mol. Graph.* **11**, 134–138.
Finzel, B. C. (1987). *J. Appl. Cryst.* **20**, 53–55.
Furey, W. & Swaminathan, S. (1996). *Methods Enzymol.* **277**, 590–620.
Ghosh, M., Meerts, I. A. T. M., Cook, A., Bergman, A., Brouwer, A. & Johnson, L. N. (2000). *Acta Cryst.* D**56**, 1085–1095.
Gonzalez, G. & Tapia, G. (1992). *FEBS Lett.* **297**, 253–256.
Hamilton, J. A., Steinrauf, L. K., Braden, B. C., Liepnieks, J., Benson, M. D., Holmgren, G., Sandgren, O. & Steen, L. (1993). *J. Biol. Chem.* **268**, 2416–2424.
Hendrickson, W. A. & Konnert, J. H. (1980). *Computing in Crystallography*, edited by R. Diamond, S. Rameseshan & K. Venkatesan, pp. 13.01–13.23. Bangalore: Indian Academy of Sciences.
Jones, T. A. & Kjeldgaard, M. (1997). *Methods Enzymol.* **277**, 173–208.
Jones, T. A., Zou, J. Y., Cowan, S. W. & Kjeldgaard, M. (1991). *Acta Cryst.* A**47**, 110–119.
Klabunde, T., Petrassi, H. M., Oza, V. B., Raman, P., Kelly, J. W. & Sacchettini, J. C. (2000). *Nature Struct. Biol.* **7**, 312–321.
Kollman, P., Dearing, A. & Kochanski, E. (1982). *J. Phys. Chem.* **86**, 1607.
Laskowski, R. A., MacArthur, M. W., Moss, D. S. & Thornton, J. M. (1993). *J. Appl. Cryst.* **26**, 283–291.
Luft, J. R., Cody, V. & DeTitta, G. T. (1992). *J. Cryst. Growth*, **122**, 181–185.
Luft, J. R. & DeTitta, G. T. (1992). *J. Appl. Cryst.* **25**, 324–325.
Luzzati, V. (1952). *Acta Cryst.* **5**, 802–810.
Miroy, J. G., Lai, Z., Lashuel, H. L., Peterson, S. A., Strang, C. & Kelly, J. W. (1996). *Proc. Natl Acad. Sci. USA*, **93**, 15051–15056.
Navab, M., Mallia, K., Kanda, Y. & Goodman, D. S. (1977). *J. Biol. Chem.* **252**, 5100–5106.
Petrassi, H. M., Klabunde, T., Sacchettini, J. W. & Kelly, J. W. (2000). *J. Am. Chem. Soc.* **122**, 2178–2192.
Pettersson, T. M., Carlstrom, A., Ehrenburg, A. & Jornval, H. (1989). *Biochem. Biophys. Res. Commun.* **158**, 341–347.
Robbins, J. (2000). *The Thyroid, A Fundamental and Clinical Text*, 8th ed, edited by L. E. Braverman & R. D. Utiger, pp. 105–120. Philadelphia: J. B. Lippincott.
Sack, J. S. (1988). *J. Mol. Graph.* **6**, 224–225.
Schormann, N., Murrell, J. R. & Benson, M. D. (1998). *Amyloid Int. J. Exp. Clin. Invest.* **5**, 175–187.
Sebastião, M. P., Merlin, G., Saraiva, M. J. & Damas, A. M. (2000). *Biochem. J.* **351**, 273–279.
Sebastião, M. P., Saraiva, M. J. & Damas, A. M. (1996). *Acta Cryst.* D**52**, 566–568.
Sebastião, M. P., Saraiva, M. J. & Damas, A. M. (1998). *J. Biol. Chem.* **273**, 24715–24722.
Steinrauf, L. K., Hamilton, J. A., Braden, B. C., Murrell, J. R. & Benson, M. D. (1993). *J. Biol. Chem.* **268**, 2425–2430.
Sunde, M., Richardson, S. J., Chang, L., Petterson, T. M., Schreiber, G. & Blake, C. C. F. (1996). *Eur. J. Biochem.* **236**, 491–499.
Sundelin, J., Melhus, H., Das, S., Eriksson, U., Lind, P., Tragardh, L., Peterson, P. A. & Rask, L. (1987). *J. Biol. Chem.* **260**, 6481–6487.
Terry, C. J., Damas, A. M., Oliveira, P., Saraiva, M. J., Alves, I. L., Costa, P. P., Matias, P. M., Sakaki, Y. & Blake, C. C. F. (1993). *EMBO J.* **12**, 735–741.
Tritish, G. L. (1972). *J. Med.* **3**, 129–145.
Wojtczak, A. (1997). *Acta Biochim. Pol.* **44**, 505–518.
Wojtczak, A., Cody, V., Luft, J. R. & Pangborn, W. (1996). *Acta Cryst.* D**52**, 758–765.
Wojtczak, A., Luft, J. R. & Cody, V. (1992). *J. Biol. Chem.* **267**, 353–357.
Wojtczak, A., Luft, J. R. & Cody, V. (1993). *J. Biol. Chem.* **268**, 6202–6206.
Wojtczak, A., Neumann, P. & Cody, V. (2001). *Acta Cryst.* D**57**, 957–967